Crystal structures of new pyrovanadates A2MnV2O7 (A = Rb, K)

Hamdi Ben Yahia, Etienne Gaudin, Jacques Darriet

Crystal Structures of New Pyrovanadates $A_2MnV_2O_7$ (A = Rb, K)

Hamdi Ben Yahia, Etienne Gaudin, and Jacques Darriet

Institut de Chimie de la Matière Condensée de Bordeaux-CNRS, Université Bordeaux 1,
87 avenue du docteur A. Schweitzer, 33608 Pessac Cedex, France

Reprint requests to Dr. E. Gaudin. Fax: (+33)540002761. E-mail: gaudin@icmcb-bordeaux.cnrs.fr

Z. Naturforsch. **2007**, *62b,* 873 – 880; received March 3, 2007

Dedicated to Dr. Bernard Chevalier on the occasion of his 60th birthday

The new compounds $A_2MnV_2O_7$ (A = K, Rb) with structures related to the melilite-type have been synthesized by a solid state reaction route. The crystal structures of $K_2MnV_2O_7$, $Rb_2MnV_2O_7$ and $KRbMnV_2O_7$ have been determined using X-ray single crystal diffraction data. The compound $K_2MnV_2O_7$ crystallizes with a melilite-type structure with tetragonal unit cell parameters a = 8.609(3), c = 5.538(4) Å and space group $P\bar{4}2_1m$. The structures of $Rb_2MnV_2O_7$ and $KRbMnV_2O_7$ are derived from the melilite-type structure with space group $P4_2/mnm$ and unit cell parameters a = 8.577(6), c = 11.809(6) Å, and a = 8.530(6), c = 11.466(5) Å, respectively. The three structures consist of $[MnV_2O_7]^{2-}$ layers perpendicular to the c axis separated by A^+ layers. The $[MnV_2O_7]^{2-}$ layers feature corner-sharing MnO_4 tetrahedra and V_2O_7 pyrovanadate units, the linkage leading to rings of five tetrahedra. The doubling of the c parameter for $Rb_2MnV_2O_7$ or $RbKMnV_2O_7$ is explained by the existence of a mirror plane perpendicular to the [001] direction between two $[MnV_2O_7]^{2-}$ layers. The A^+ alkali cations occupy distorted square antiprisms of oxygen atoms in $K_2MnV_2O_7$ and distorted square prisms of oxygen atoms in $Rb_2MnV_2O_7$and $RbKMnV_2O_7$.

Key words: Vanadate, Melilite, Crystal Chemistry, Single Crystal X-Ray Diffraction, Oxides

Introduction

Most of the minerals of the melilite group are silicates with the general formula $^{[8]}A_2^{[4]}B^{[4]}Si_2O_7$ ([N] = coordination number). Among them, one can find the akermanite $Ca_2MgSi_2O_7$ [1], the gehlenite $Ca_2Al(AlSi)O_7$ [2], the okayamalite $Ca_2B(BSi)O_7$ [3] the hardystonite $Ca_2ZnSi_2O_7$ [4], the gugiaite $Ca_2BeSi_2O_7$ [5], and the melilite $(Ca,Na)_2(Mg,Fe,Al)(AlSi)O_7$ [6]. Many melilite-type compounds have been synthezised with a wide range of chemical compositions, the general formula becoming $A_2BC_2X_7$ where A is a large cation such as Ca, Sr, Ba, Na, K, Y, lanthanides (La–Er), Pb, Bi; B is a small four coordinated cation such as Be, Mg, Mn, Fe, Co, Cu, Zn, Cd, Al, Ga, Si; C = Cr, Al, Ga, Si, Ge, B, V, and X = O, F, S, N. The melilite-type structure was first determined by Warren (1930) [1]. The structure has a tetragonal symmetry, space group $P\bar{4}2_1m$, and consists of BC_2O_7 layers parallel to (001) made of corner-sharing BO_4 and CO_4 tetrahedra. The cations A are lying between these layers in distorted square antiprisms of oxygen atoms. Recently, Tyutyunnik *et al*. have synthesized $Na_2ZnV_2O_7$, the first vanadate crystallizing in the melilite-type structure [7].

In the past only few vanadate compounds having structures closely related to the melilte-type have been prepared. The compounds $(NH_4)_2VOV_2O_7$ [8], $K_2VOV_2O_7$ [9], $Rb_2VOV_2O_7$ [10], and $KBaCuClV_2O_7$ [11] crystallize in the fresnoite-type structure which is very similar to the melilite-type, except that the V_2O_7 pyrogroups all point in the same direction and the V^{4+} and Cu^{2+} coordination polyhedra are square pyramids instead of the usual tetrahedra. They all have tetragonal cell parameters with space group $P4bm$ and with a ranging from 8.8581(13) to 8.9229(10) Å and c ranging from 5.215(5) to 5.5640(5) Å. A different variation of the melilite-type structure is observed for $K_2MgV_2O_7$ [12], which crystallizes in space group $P4_2/mnm$ with cell parameters a = 8.38(2) and c = 11.36(2) Å. The main difference between the $K_2MgV_2O_7$ and the melilite-type structures is the doubling of the lattice constant c explained by the existence of a mirror plane perpendicular to the [001] direction between two MgV_2O_7 layers. This induces a change from $P\bar{4}2_1m$ to $P4_2/mnm$ symmetry. This structural variation is only

0932–0776 / 07 / 0700–0873 $ 06.00

observed for phosphates and vanadates [12 – 15]. Notably, $P\bar{4}2_1m$ and $P4_2/mnm$ are both subgroups of space group P4/*mbm*. No compound of the melilite group crystallizes in this space group.

Crystals of the new phase $K_2MnV_2O_7$ were obtained during fast melting of a vanadate powder with the composition $KMnVO_4$. In a recent paper the crystal structure of $KMnVO_4$ has been solved and shown to be an oxygen-deficient perovskite [16].

The aim of this work is to discuss the structural effects of the partial or complete substitution of K^+ for Rb^+ on the A positions of the compounds of general formula $A_2MnV_2O_7$, in order to contribute to a better insight into the crystal chemistry of the divanadates $A_2BV_2O_7$.

Experimental Section

$K_2MnV_2O_7$ was prepared by solid state reaction from a stoichiometric mixture of KVO_3 and MnO. KVO_3 was obtained by heating a 1 : 1 mixture of K_2CO_3 and V_2O_5 at 550 °C for 6 h. The mixture was put in a gold tube which was sealed under vacuum in a silica tube and then heated at 450 °C for 24 h and at 500 °C for 12 h. After grinding a further heating of the mixture at 500 °C for 18 h led to a mixture of three phases: $K_2MnV_2O_7$, KVO_3, and MnO. Different treatments (time and temperature) did not improve the results. As KVO_3 is soluble in water, the powder sample was washed to obtain $K_2MnV_2O_7$ as major phase (Fig. 1). Attempts to prepare single crystals of $K_2MnV_2O_7$ by melting the sample powder were unsuccessful. Subsequently, a 1 : 1 mixture of KVO_3 and MnO was prepared. By fast heating of this starting mixture at 950 °C followed by slowly decreasing the temperature at the rate of 5 °C h^{-1} to r. t., a mixture of yellow, orange and green crystals corresponding to $KMnVO_4$, $K_2MnV_2O_7$, and MnO, respectively, was obtained.

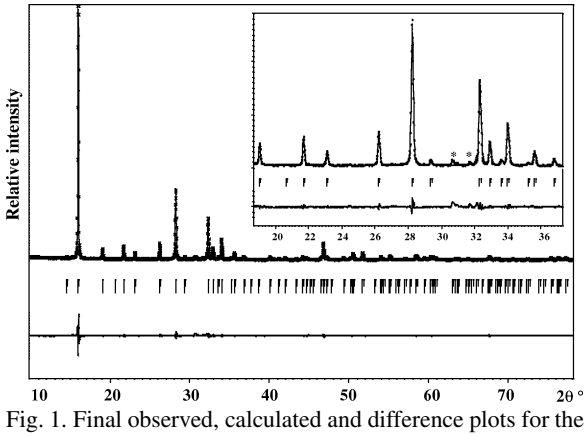

Fig. 1. Final observed, calculated and difference plots for the XRPD profile refinement of $K_2MnV_2O_7$ (peaks marked with an asterisk indicate impurities).

$Rb_2MnV_2O_7$ powder and crystals were prepared exactly in the same way as $K_2MnV_2O_7$. We used $RbVO_3$ instead of KVO_3. $RbVO_3$ was obtained by heating a 1 : 1 mixture of Rb_2CO_3 and V_2O_5 at 700 °C for 10 h.

$KRbMnV_2O_7$ was prepared by solid state reaction from a stoichiometric mixture of KVO_3, $RbVO_3$ and MnO. The mixture was put in a gold tube which was sealed under vacuum in a silica tube and then heated at 500 °C for 48 h with intermittent grinding. This led to a mixture of $KRbMnV_2O_7$, $K_{1-x}Rb_xVO_3$, and MnO. The heating of this mixture at 950 °C for 2 h and the slow cooling at the rate of 5 °C h^{-1} to 700 °C and at 10 °C h^{-1} to r. t. enabled us to obtain several crystals of $KRbMnV_2O_7$.

X-Ray diffraction measurements

Crystals of the title compounds suitable for single crystal X-ray diffraction were selected on the basis of the size and the sharpness of the diffraction spots. In the case of $Rb_2MnV_2O_7$, the quality of the single crystals was really poor, and this explains the high internal R value (see Table 1). A similar problem was encountered for $KRbMnV_2O_7$. The data collections were carried out on an Enraf-Nonius Kappa CCD diffractometer using MoK_α radiation. Data processing and all refinements were performed with the JANA2000 program package [17]. A Gaussian-type absorption correction was applied, and the shapes were determined with the video microscope of the Kappa CCD. Details of data collection are summarized in Table 1.

Structure refinement

The extinction conditions observed for $K_2MnV_2O_7$ agree with the space group $P\bar{4}2_1m$. Most of the atomic positions were found by Direct Methods using SIR97 [18]. With anisotropic displacement parameters, the final residual factors converged to $R(F) = 0.025$ and $wR(F^2) = 0.055$ for 34 refined parameters, 832 observed reflections and difference-Fourier residues in the range between -0.33 and $+0.32$ e Å^{-3}. The Flack parameter refined to 0.01(4).

The lattice of $Rb_2MnV_2O_7$ has tetragonal geometry. The observed systematic extinctions agree with space group $P4_2/mnm$. The structure was solved by Direct Methods using SHELXS-97 [19], which revealed the heavy atom positions. Several difference-Fourier syntheses allowed us to localize the oxygen atom positions. This refinement led to the residual factors $R(F) = 0.042$ and $wR(F^2) = 0.088$ for 36 refined parameters, 455 observed reflections and difference-Fourier residues in the range between -1.06 and $+1.43$ e Å^{-3}.

The extinction conditions observed for $RbKMnV_2O_7$ agree with the space group $P4_2/mnm$ already used for the

Table 1. Crystallographic data and structure refinement for $K_2MnV_2O_7$, $Rb_2MnV_2O_7$, and $RbKMnV_2O_7$.

Formula	$K_2MnV_2O_7$	$Rb_2MnV_2O_7$	$RbKMnV_2O_7$
Crystals	orange block	yellow block	yellow block
MW, g mol^{-1}	347	439.7	393.4
Crystal system		tetragonal	
space group	$P\bar{4}2_1m$	$P4_2/mnm$	$P4_2/mnm$
$a = b$, Å	8.609(3)	8.577(6)	8.530(6)
c, Å	5.538(4)	11.809(6)	11.466(5)
V, Å^3	410.4(4)	868.7(10)	834.3(9)
Z	2	4	4
Density calc, g cm^{-3}	2.81	3.36	3.13
Temperature, K		293(1)	
Diffractometer		Enraf-Nonius KappaCCD	
Monochromator		Oriented graphite	
Radiation; λ, Å		MoK_α; 0.71069	
Scan mode		CCD scan	
$h\,k\,l$ range	$-13 < h < 13$	$-12 < h < 11$	$-12 < h < 12$
	$-12 < k < 13$	$-12 < k < 12$	$-12 < k < 12$
	$-8 < l < 8$	$-17 < l < 17$	$-17 < l < 16$
θ_{min} / θ_{max}, deg	3.35 / 34.99	2.94 / 31.95	4.78 / 2.02
Linear absorption coeff. (mm^{-1})	4.8	14.7	10.0
Absorption correction		Gaussian	
T_{min} / T_{max}	0.477 / 0.716	0.499 / 0.816	0.379 / 0.837
No. of reflections	8856	14505	12515
R_{int}	0.067	0.176	0.140
No. of independent reflections	976	849	819
Reflections used [$I \geq 3\sigma(I)$]	832	455	540
Refinement		F^2	
F(000), e	330	804	732
No. of refined parameters	34	36	37
R factors $R(F)$ / $wR(F^2)$	0.025 / 0.055	0.042 / 0.088	0.044/0.100
x (Flack)	0.01(4)	–	–
g. o. f.	1.09	1.23	1.52
Weighting scheme		$w = 1/(\sigma^2(I) + 0.0009I^2)$	
Diff. Fourier residues, e Å^{-3}	−0.33 / +0.32	−1.06 / +1.43	−0.76 / +0.85

Table 2. Atom positions and isotopic displacement parameters for $K_2MnV_2O_7$, $Rb_2MnV_2O_7$, and $KRbMnV_2O_7$.

Atoms	Occupancy	Site	x	y	z	U_{eq} (Å^2)
$K_2MnV_2O_7$						
K	1	4*e*	0.83871(5)	1/2 + x	0.50737(14)	0.02491(13)
Mn	1	2*a*	0	0	0	0.01567(12)
V	1	4*e*	0.14046(4)	0.35954(4)	0.05876(8)	0.01252(8)
O1	1	8*f*	0.0876(2)	0.18543(18)	0.1802(3)	0.0215(4)
O2	1	2*c*	0	1/2	0.1610(6)	0.0188(6)
O3	1	4*e*	0.1452(2)	0.3548(2)	0.7616(4)	0.0283(5)
$Rb_2MnV_2O_7$						
Rb1	1	4*g*	0.32119(10)	x	1/2	0.0375(3)
Rb2	1	4*f*	0.85079(10)	$-x$	1/2	0.0310(3)
Mn	1	4*d*	1/2	0	1/4	0.0245(4)
V	1	8*j*	0.63961(11)	$-x$	0.28601(15)	0.0224(3)
O1	1	16*k*	0.5881(5)	0.1826(5)	0.3395(5)	0.0299(16)
O2	1	4*e*	1/2	1/2	0.3380(4)	0.0268(13)
O3	1	8*j*	0.6411	$-x$	0.1472(7)	0.034(2)
$KRbMnV_2O_7$						
K1	0.572(7)	4*g*	0.31980(13)	x	1/2	0.0342(5)
Rb1	0.428	4*g*	0.3198	x	1/2	0.0342
K2	0.428	4*f*	0.85335(11)	$-x$	1/2	0.0271(4)
Rb2	0.572	4*f*	0.8534	$-x$	1/2	0.0271
Mn	1	4*d*	1/2	0	1/4	0.0161(3)
V	1	8*j*	0.64028(9)	$-x$	0.28842(10)	0.0136(2)
O1	1	16*k*	0.5888(4)	0.1815(3)	0.3446(3)	0.0201(9)
O2	1	4*e*	1/2	1/2	0.3432(6)	0.0191(15)
O3	1	8*j*	0.6410(4)	$-x$	0.1458(4)	0.0266(12)

Table 3. Final displacement parameters for $K_2MnV_2O_7$, $Rb_2MnV_2O_7$, and $KRbMnV_2O_7$.

Atoms	U_{11}	U_{22}	U_{33}	U_{12}	U_{13}	U_{23}
$K_2MnV_2O_7$						
K	0.0267(2)	U_{11}	0.0213(3)	−0.0081(2)	0.00382(16)	0.00382(16)
Mn	0.01199(15)	U_{11}	0.0230(3)	0	0	0
V	0.01164(11)	U_{11}	0.01428(19)	0.00102(14)	0.00057(11)	−0.00057(11)
O1	0.0236(8)	0.0128(6)	0.0282(9)	−0.0043(6)	−0.0038(6)	−0.0006(6)
O2	0.0184(8)	U_{11}	0.0195(15)	0.0080(11)	0	0
O3	0.0343(8)	U_{11}	0.0161(9)	0.0080(13)	0.0025(7)	−0.0025(7)
$Rb_2MnV_2O_7$						
Rb1	0.0409(5)	U_{11}	0.0307(7)	−0.0150(6)	0	0
Rb2	0.0314(4)	U_{11}	0.0302(7)	0.0057(5)	0	0
Mn	0.0215(6)	U_{11}	0.0306(10)	0	0	0
V	0.0214(5)	U_{11}	0.0244(7)	−0.0003(5)	0.0007(4)	−0.0007(4)
O1	0.032(2)	0.020(2)	0.038(4)	−0.006(3)	0.0003(19)	0.0041(19)
O2	0.027(2)	U_{11}	0.027(3)	0.0060(19)	0	0
O3	0.041(3)	U_{11}	0.021(5)	0.009(4)	0.002764	−0.002764
$KRbMnV_2O_7$						
K1/Rb1	0.0374(7)	U_{11}	0.0279(9)	−0.0175(7)	0	0
K2/Rb2	0.0269(5)	U_{11}	0.0275(8)	0.0050(5)	0	0
Mn	0.0121(4)	U_{11}	0.0242(7)	0	0	0
V	0.0118(3)	U_{11}	0.0172(5)	0.0009(4)	0.0000(3)	0.0000(3)
O1	0.0217(17)	0.0115(17)	0.027(3)	−0.004(2)	−0.0037(15)	0.0009(15)
O2	0.0173(16)	U_{11}	0.0226(19)	0.0027(14)	0	0
O3	0.0297(19)	U_{11}	0.021(3)	0.003(3)	0.002149	−0.002149

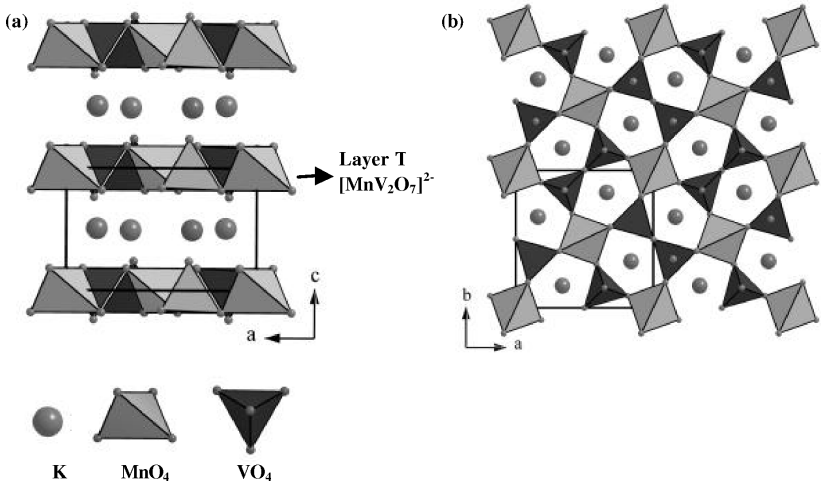

Fig. 2. Projection of the crystal structure of $K_2MnV_2O_7$ (a) onto the *ac* plane and (b) onto the *ab* plane.

refinement of the homologous compound $Rb_2MnV_2O_7$. The atomic positions of the latter were used as a starting model for the refinement. The rubidium atom in the $4f$ position was replaced by a potassium atom to get the correct formula $RbKMnV_2O_7$. At this stage the refinement led to residual factors of $R(F) = 0.194$ and $wR(F^2) = 0.430$ with large negative displacement parameters for Rb (0.067 Å^2) and K, respectively. Attempts to solve the structure with fully ordered sites failed; therefore the structure was refined with introduction of K/Rb disorder on the $4g$ and $4f$ positions. With anisotropic displacement parameters, the final residual factors converged to $R(F) = 0.044$ and $wR(F^2) = 0.100$ for 37 refined parameters, 540 observed reflections and difference-Fourier residues in the range between −0.76 and +0.85 e Å^{-3}. The refined atomic positions and anisotropic displacement parameters (ADPs) of the different phases are given in Tables 2 and 3, respectively.

Further details may be obtained from: Fachinformationszentrum Karlsruhe, D-76344 Eggenstein-Leopoldshafen (Germany), by quoting the Registry No's. CSD–417890 ($Rb_2MnV_2O_7$), CSD–417891 ($KRbMnV_2O_7$), and CSD–417892 ($K_2MnV_2O_7$).

Results and Discussion

The crystal structure of $K_2MnV_2O_7$ is isotypic to the melilite-type structure consisting of alternating MnV_2O_7 and K layers (Fig. 2a). The MnV_2O_7 lay-

$K_2MnV_2O_7$		$Rb_2MnV_2O_7$		$KRbMnV_2O_7$	
distance		distance		distance	
Mn–O1 (×4)	2.0279(17)	Mn–O1 (×4)	2.035(4)	Mn–O1 (×4)	2.036(3)
V–O3	1.646(2)	V–O3	1.640(7)	V–O3	1.635(5)
V–O1 (×2)	1.7047(17)	V–O1 (×2)	1.709(4)	V–O1 (×2)	1.709(3)
V–O2	1.8014(11)	V–O2	1.801(3)	V–O2	1.805(2)
	⟨1.7142⟩		⟨1.714⟩		⟨1.714⟩
K–O2	2.745(2)	Rb1–O3 (×2)	2.791(5)	K1/Rb1–O3 (×2)	2.729(4)
K–O1 (×2)	2.7770(19)	Rb1–O2 (×2)	2.892(5)	K1/Rb1–O2 (×2)	2.821(4)
K–O3	2.787(2)	Rb1–O1 (×4)	3.201(5)	K1/Rb1–O1 (×4)	3.136(3)
K–O3 (×2)	2.994(2)		⟨3.021⟩		⟨2.955⟩
K–O1 (×2)	3.1008(18)				
	⟨2.9094⟩	Rb2–O1 (×4)	2.958(4)	K2/Rb2–O1 (×4)	2.891(3)
		Rb2–O3 (×4)	3.037(5)	K2/Rb2–O3 (×4)	2.969(4)
			⟨2.997⟩		⟨2.930⟩
angle		angle		angle	
O1–Mn–O1 (×4)	104.01(7)	O1–Mn–O1 (×4)	105.66(17)	O1–Mn–O1 (×4)	106.48(15)
O1–Mn–O1 (×2)	121.05(7)	O1–Mn–O1 (×2)	117.4(2)	O1–Mn–O1 (×2)	115.63(19)
	⟨109.69⟩		⟨109.57⟩		⟨109.53⟩
O1–V–O2 (×2)	106.67(8)	O1–V–O2 (×2)	107.16(18)	O1–V–O2 (×2)	106.76(15)
O1–V–O1	108.30(9)	O1–V–O1	108.9(2)	O1–V–O1	108.41(19)
O2–V–O3	110.35(12)	O2–V–O3	110.59(15)	O2–V–O3	110.66(12)
O1–V–O3 (×2)	112.26(9)	O1–V–O3 (×2)	111.4(2)	O1–V–O3 (×2)	111.99(17)
	⟨109.41⟩		⟨109.43⟩		⟨109.42⟩
V–O2–V	143.3(2)	V–O2–V	140.1(3)	V–O2–V	139.3(3)
V–O1–Mn	126.68(10)	V–O1–Mn	126.2(4)	V–O1–Mn	124.9(3)
BVS		BVS		BVS	
Mn	2.10	Mn	2.06	Mn	2.06
V	5.14	V	5.14	V	5.16
K	1.05	Rb1	1.16	K1/Rb1	1.02
		Rb2	1.10	K2/Rb2	1.13

Table 4. Interatomic distances (Å), angles (deg) and bond valence sums (BVS)[a] for $K_2MnV_2O_7$, $Rb_2MnV_2O_7$, and $KRbMnV_2O_7$.

[a] BV = $e^{(r_0-r)/b}$ with the following parameters [23]: b = 0.37 and r_0 (Mn^{II}–O) = 1.790, r_0 (V^V–O) = 1.803, r_0 (K–O) = 2.132 and r_0 (Rb–O) = 2.263 Å.

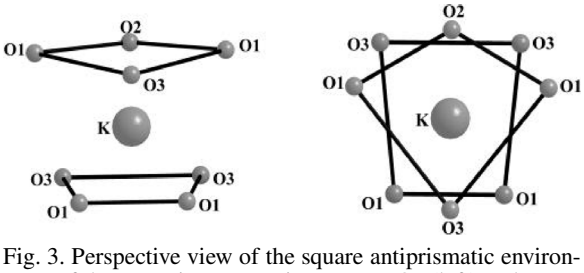

Fig. 3. Perspective view of the square antiprismatic environment of the potassium atoms in $K_2MnV_2O_7$ (left) and a projection of the crystal structure along [001] (right).

ers contain corner-sharing MnO_4 tetrahedra and V_2O_7 pyrovanadate units (two corner-sharing VO_4 tetrahedra) that form rings of five tetrahedra (Fig. 2b). The eight-coordinated cations K are positioned between these layers. The interatomic distances for the MnO_4, VO_4 and KO_8 polyhedra are listed in Table 4. The MnO_4 tetrahedra contain four regular Mn–O bonds of 2.028(2) Å very close to the value of 2.04 Å estimated from the effective ionic radii of Mn^{2+} and O^{2-} [20]. A comparable Mn–O distance has been reported for the analogous silicate $Sr_2MnSi_2O_7$ [21]. The large O–Mn–O angles of 121.05(7)° indicate that the MnO_4 tetrahedron is flattened along the [001] direction. Two neighboring VO_4 units share an O2 atom to form the pyrovanadate unit $[V_2O_7]^{4-}$. This induces an elongated V–O2 distance of 1.8014(11) Å, typical of divanadate entities in which the longer distance characterizes the V–O–V bridge [7 – 12]. In the VO_4 tetrahedron the average V–O distance of 1.714 Å is slightly lower than the value of 1.735 Å expected from the sum of the effective ionic radii. No significant deviation from the ideal tetrahedral angle of 109.5° is observed. The O–V–O angles range from 106.67(17) to 112.26(9)° with an average value of 109.4°. The O–V–O angles and the V–O distances are nearly equal to those found in $Na_2ZnV_2O_7$ (distances: 1.649(5), 1.725(4) (×2), and 1.802(3) Å; angles: 106.2(3), 107.0(2), 111.9(3), and 112.2(2)°) [7].

The coordination polyhedron around the A-site K atom is a distorted square antiprism (Fig. 3). There are four short K–O distances ranging from 2.745(2) to 2.787(2) Å and four stretched distances ranging from 2.994(2) to 3.101(2) Å, giving an average value of

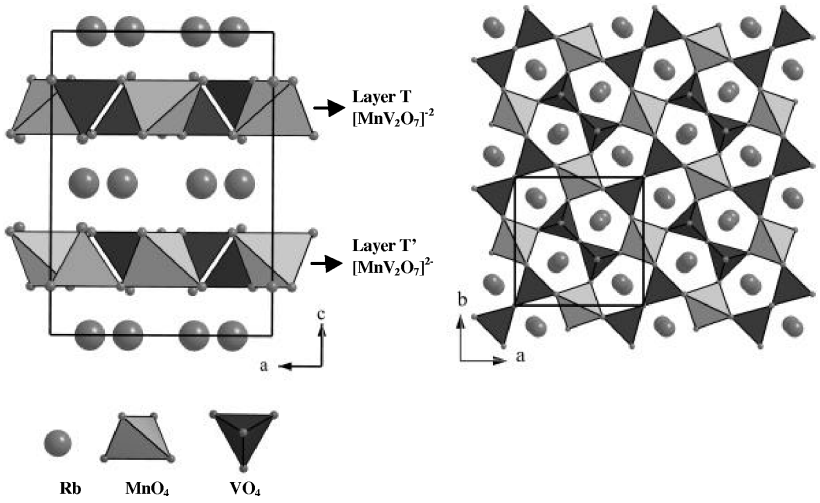

Fig. 4. Projection of the crystal structure of $Rb_2MnV_2O_7$ onto the *ac* plane (left) and onto the *ab* plane (right).

2.909 Å consistent with the Shannon Table (d_{K-O} = 2.93 Å). The calculations of the bond valence sums (BVS) for Mn^{2+}, V^{5+}, K^+ confirm the charge balance (*i. e.*, BVS = 2.10, 5.14 and 1.05 for Mn^{2+}, V^{5+} and K^+, respectively) [22, 23].

Projection views onto the (010) and (001) planes of the $Rb_2MnV_2O_7$ structure are displayed in Fig 4. The unit cell parameter c of the $Rb_2MnV_2O_7$ structure is larger than that of melilite $K_2MnV_2O_7$ by a factor of approximately two. The addition of a symmetry element to the space group $P\bar{4}2_1m$ leads to space group $P4_2/mnm$. As a result, the unit cell of the rubidium manganese vanadate contains two layers of tetrahedral $[MnV_2O_7]^{2-}$, T and T' (Fig. 4, left), which are related by the mirror plane, instead of only one layer T in $K_2MnV_2O_7$ (Fig. 2a). The MnV_2O_7 layers are similar to those observed for $K_2MnV_2O_7$, consisting of corner-sharing MnO_4 and VO_4 tetrahedra, the latter forming V_2O_7 pyrogroups. The Rb^+ cation layers are situated between the $[MnV_2O_7]^{2-}$ layers. As expected, when rubidium is substituted for potassium a slight increase of the interlayer space is observed with $c/2$ = 5.905 Å for $Rb_2MnV_2O_7$ and c = 5.538 Å for $K_2MnV_2O_7$. The main difference between the two compounds is found in the interlayer alkali cation environment. Indeed, in $K_2MnV_2O_7$ the potassium atoms occupy only one site (4*e*) with a square antiprismatic coordination (Fig. 3), whereas in $Rb_2MnV_2O_7$ the rubidium atoms occupy two different sites (4*g* and 4*f* for Rb1 and Rb2, respectively) with a distorted square prismatic coordination (Fig. 5). The Rb1 polyhedron is more distorted than that of Rb2. The distances Rb–O

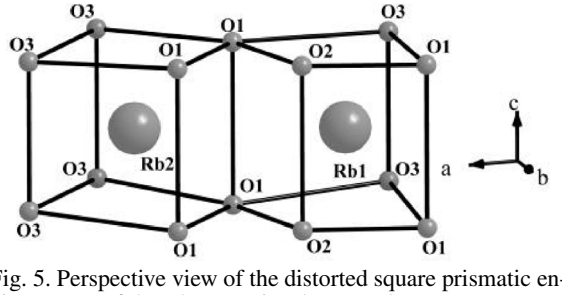

Fig. 5. Perspective view of the distorted square prismatic environments of the Rb atoms in $Rb_2MnV_2O_7$.

range from 2.791(5) to 3.201(5) Å and from 2.958(4) to 3.037(5) Å giving an average distance of 3.02 and 3.00 Å and a bond valence sum of 1.16 and 1.10 for Rb1 and Rb2, respectively. This is in agreement with the sum of ionic radii of 3.03 Å and the charge balance of +1. The short distance Rb1–O3 of 2.791(5) Å is attributed to the fact that the O3 position is shared by the $Rb1O_8$ and VO_4 polyhedra. Indeed, in order to obtain an acceptable Rb–O3 distance the V–O3 distance is compressed along the [001] direction to a value of 1.646(2) Å. This steric strain is reflected by the relatively large anisotropic displacement parameters (U_{11} = U_{22} = 0.041 Å^2) for the O3 position and (U_{11} = U_{22} = 0.0409 Å^2) for the Rb1 position (Table 3).

As in $K_2MnV_2O_7$, in $Rb_2MnV_2O_7$ the MnO_4 and V_2O_7 units form rings of five tetrahedra (Fig. 6) with no significant changes in the V–O and Mn–O distances and in the V–O2–V and V–O1–Mn bridging angles (Table 4). The bond valence sums (BVS) of 2.06 and 5.14 are in agreement with the values expected for Mn^{2+} and V^{5+}, respectively [22, 23].

Table 5. Compounds illustrating the effect of the substitution in the melilite-type structure.

Melilite-type $P\bar{4}2_1m$		Derivative of melilite-type $P4_2/mnm$	
$K_2MnV_2O_7$	this work	$K_2MgV_2O_7$	ref. [12]
		$K_2ZnP_2O_7$	ref. [13]
		$KRbMnV_2O_7$	this work
		$Rb_2MnV_2O_7$	this work
$Na_2ZnV_2O_7$	ref. [7]	$Na_2ZnP_2O_7$	ref. [13]
		$Na_2CoP_2O_7$	ref. [14]
		$Ag_2ZnP_2O_7$	ref. [15]

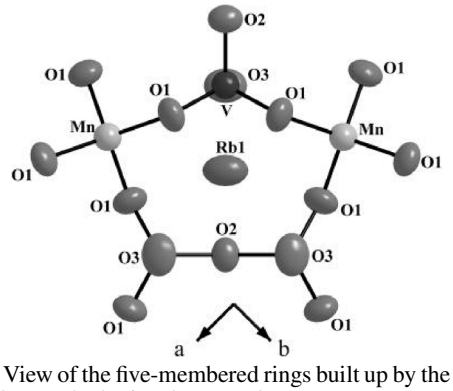

Fig. 6. View of the five-membered rings built up by the MnO_4 and VO_4 tetrahedra in $Rb_2MnV_2O_7$.

These results indicate that there is no change in the dimension of the sheets of tetrahedra and accordingly no significant change in the lattice parameter a (Table 1).

The mixed potassium rubidium divanadate $RbKMnV_2O_7$ is isostructural to $Rb_2MnV_2O_7$. The difference between the two compounds is the appearance of K/Rb disorder in the Rb1 and Rb2 positions which induces a more relaxed structure. This is mainly reflected by the lower values of the anisotropic displacement parameters of all atoms in $RbKMnV_2O_7$ (Table 3). We can also see that the MnO_4 tetrahedra are less flattened in the [001] direction (d_{Mn-O} = 2.036 Å and O1–Mn–O1 = 115.63°) than in $Rb_2MnV_2O_7$ (d_{Mn-O} = 2.035 Å and O1–Mn–O1 = 117.4°) or in $K_2MnV_2O_7$(d_{Mn-O} = 2.028 Å and O1–Mn–O1 = 121.05°) (Table 4). Bindi *et al*. reported the observation that the greater the size of the tetrahedral cations with respect to the cations A, the greater the structural misfit leading to the incommensurate structure is found [24]. We can then assume that the structural transition from the melilite-type (space group $P\bar{4}2_1m$) to the closely related structure of $Rb_2MnV_2O_7$ and $KRbMnV_2O_7$ (space grop $P4_2/mnm$) proceeds by an analogous mechanism. When the size of the tetrahedral cations for B and/or C decreases (with the same cation A) or the size of the cations A increases (no change in B and C sizes) a phase transition occurs. For example, in $K_2MnV_2O_7$ when Mg^{2+} (r_{ionic} = 0.57 Å [20]) is substituted for Mn^{2+} (0.66 Å), Zn^{2+} (0.60 Å) and P^{5+} (0.17 Å) for Mn^{2+} (0.66 Å) and V^{5+} (0.355 Å) or Rb^+ (1.61 Å) for K^+ (1.51 Å), this structural transition is observed (see Table 1). The same behavior is observed for $Na_2ZnV_2O_7$ when phosphorus is substituted for vanadium, the size of the other cations being almost constant (Table 5).

[1] B. E. Warren, *Z. Kristallogr*. **1930**, *74*, 131 – 138.
[2] F. Raaz, *Mineralog. und Petrogr. Mitt*. **1932**, *42*, 72 – 78.
[3] S. Matsubara, R. Miyawaki, A. Kato, K. Yokoyama, A. Okamoto, *Mineral. Mag*. **1998**, *62*, 703 – 706.
[4] B. E. Warren, O. R. Trautz, *Z. Kristallogr*. **1930**, *75*, 525 – 528.
[5] M. Kimata, H. Ohashi, *Neues Jb. Miner. Monat*. **1982**, *143*, 210 – 222.
[6] V. I. Mokeeva, E. S. Makarov, *Geokhimiya* **1979**, *10*, 1541 – 1544.
[7] A. P. Tyutyunnik, V. G. Zubkov, L. L. Surat, B. V. Slobodin, G. Svensson, *Powder Diffr*. **2005**, *20*, 189 – 192.
[8] K.-J. Range, R. Zintl, *Z. Naturforsch*. **1988**, *B43*, 309 – 317.
[9] J. Galy, A. Carpy, *Acta Crystallogr*. **1975**, *B31*, 1794 – 1795.
[10] M.-L. Ha-Eierdanz, U. Müller, *Z. Anorg. Allg. Chem*. **1992**, *613*, 63 – 66.
[11] F.-D. Martin, H. Müller-Buschbaum, *Z. Naturforsch*. **1994**, *B49*, 355 – 359.
[12] E. V. Murashova, Yu. A. Velikodnyi, V. K. Trunov, *Russ. J. Inorg. Chem*. **1988**, *33*, 904 – 905.
[13] Yu. F. Shepelev, M. A. Petrova, A. S. Novikova, A. E. Lapshin, *Glass Phys. Chem*. **2002**, *28*, 317 – 321.
[14] F. Sanz, C. Parada, J. M. Rojo, C. Ruiz-Valero, R. Saez-Puche, *J. Solid State Chem*. **1999**, *145*, 604 – 611.
[15] I. Belharouak, C. Parent, P. Gravereau, J. P. Chaminade, G. le Flem, B. Moine, *J. Solid State Chem*. **2000**, *149*, 284 – 291.
[16] H. Ben Yahia, E. Gaudin, J. Darriet, M. Banks, M. H. Whangbo, *Chem. Mater*, in press.
[17] V. Petříček, M. Dušek, L. Palatinus, JANA2000, The Crystallographic Computing System, Institute of Physics, Praha (Czech Republic) **2000**.

[18] A. Altomare, M. C. Burla, M. Camalli, G. L. Cascarano, C. Giacovazzo, A. Guagliardi, A. G. G. Moliterni, G. Polidori, R. Spagna, SIR97, *J. Appl. Crystallogr.* **1999**, *32*, 115 – 119.
[19] G. M. Sheldrick, SHELXS-97, Universität Göttingen, Göttingen (Germany) **1997**.
[20] R. D. Shannon, *Acta Crystallogr.* **1976**, *A32*, 751 – 767.
[21] M. Kimata, *Neues Jb. Miner. Monat.* **1985**, *2*, 83 – 96.
[22] I. D. Brown, D. Altermatt, *Acta Crystallogr.* **1985**, *B41*, 244 – 247.
[23] N. E. Brese, M. O'Keeffe, *Acta Crystallogr.* **1991**, *B47*, 192 – 197.
[24] L. Bindi, M. Dusek, V. Petricek, P. Bonazzi, *Acta Crystallogr.* **2006**, *B62*, 1031 – 1037.